Geometrical and Textural Features Extraction for Honey Plants Pollen Recognition

Lyubomir Zaykov [1], Diana Tsankova [1]

[1] University of Food Technologies, 26, Maritsa Blvd, Plovdiv, Bulgaria

Abstract – The aim of the study is to investigate the extraction of features from microscopic images of honey plants pollen for classifying honey based on its botanical origin. Pollens from black locust, linden, lavender, canola and thistle are used. The color image of the pollen grain is converted into a gray image, from which classification features are extracted using popular texture recognition methods - Gabor filter, gray level co-occurrence matrix and local binary patterns. The extracted textural features are then processed with the principal component analysis method for dimensionality reduction and removal of correlated data. Geometric features related to the shape of the pollen grain are extracted from the binarized image. Through linear discriminant analysis, four classifiers are synthesized based on the textural and geometric features. To improve their performance, three hybrid structures mixing textural and geometric features are proposed. A comparative analysis of the performance of all seven linear classifiers is performed using a leave-one-out-cross-validation test. The best success rate obtained is 96%. The efficacy of the proposed algorithms is assessed through simulations conducted using the MATLAB programming language.

Keywords – Pollen recognition, features extraction, shape of pollen grain, Gabor filter, GLCM, LBP, PCA, LDA.

The article is published with Open Access at https://www.temjournal.com/

1. Introduction

Part of the analysis for honey authentication involves determining its botanical origin, i.e. the source of flower nectar. International legislation [1], [2] permits the inclusion of information regarding the botanical origin of honey on the product label, provided that the honey is derived entirely or predominantly from the specified plant source. The commercial valuation of honey is significantly influenced by its botanical origin. Quality analysis, therefore, encompasses the identification of the honey's botanical provenance.

Based on whether the nectar is sourced from the flowers of a single plant species or multiple species, nectar honey can be classified accordingly as monofloral or polyfloral [3]. It is practically impossible to collect nectar from only one type of plant, and therefore honey obtained from the nectar of many plants, but one must prevail among them, is considered monofloral. Certain countries have established and enacted national regulations or criteria pertaining to the defining characteristics of monofloral honey [4]. As defined by Bulgarian regulatory documents [3], the pollen profile of monofloral bee honey must contain pollen grains from the respective plant species in proportions of at least 15% for lavender, 30% for acacia (black locust), and 40% for other types of honey. For commercial purposes, Bulgarian monofloral honey is mainly produced from acacia, linden, lavender, rapeseed (canola) and thistle.

Generally, pollen analysis is used to determine the botanical origin of honey [4], [5]. Some of its limitations can be overcome by further research on the sensory and physicochemical properties of honey [5], [6], [7], [8], [9], [10]. Unlike other analyses spectroscopy is a non-invasive, relatively easy and quick method that can be an auxiliary method to the normative ones for clarifying the botanical origin of honey [11], [12], [13], [14], [15].

Pollen analysis continues to be the principal method for determining the botanical origin of honey.

However, it presents significant challenges, including its labor-intensive nature, the substantial time required, the necessity for highly skilled personnel and expert knowledge, and its unsuitability for automation.

The technological activities and time required for the preparation of the microscope slides (centrifugation of honey solutions, treatment with chemicals and drying) are relatively constant standardized quantities. To interpret the microscopic images, expert knowledge is needed to recognize the pollen of honey plants, as well as to distinguish it from other organic microparticles that could get into the honey from the air through the bee's body. At this stage, experts can be assisted by a computerized system to recognize and count pollen images, and as a result, to make a decision about the botanical origin of honey and pollen.

Traditional methods for pollen recognition have relied on geometric and textural features analyzed through various classifiers, including linear discriminant analysis (LDA) and artificial neural networks (ANNs). Treloar et al. [16] have achieved an average classification success rate of 95% by employing geometric features such as ovality, perimeter, and area of the pollen grain, utilizing an LDA-based classifier to distinguish among 12 different pollen types. Garcia et al. [17] have proposed a classifier based on a hidden Markov model trained on pollen grain contour data. It has achieved an average success rate of 98.8% classifying 17 different types of pollen from 11 honey plant families.

Marcos et al. [18] have used a number of different textural methods to extract informative features of pollen texture, including: gray level co-occurrence matrix (GLCM); local binary patterns (LBP); log-Gabor filters; discrete moments of Chebyshev; and others. They have used a database of 1800 samples comprising 15 different taxa. Their approach has correctly identified 95% of samples. Gray level co-occurrence matrix applied to texture features extraction and a classifier using an ANN, have been employed in [19] to identify 10 distinct types of pollen in honey based on reference pollen from various plant species. The model has achieved a recognition rate of 88%.

In their study, Rodríguez-Damian et al. [20] have employed a combined analysis of shape and texture to distinguish between closely related pollen species. They have utilized three standard classifiers - the minimum distance classifier based on Mahalanobis distance, the multilayer perceptron, and the support vector machine (SVM) classifier - to achieve a classification accuracy of 89% for pollen grains.

A combination of 3 types of features (derived from shape, texture and aperture) has been used in [21] to create SVMs and random forest classifiers. The texture features extraction methods have included: Gabor filter (GF), fast Fourier transform, histogram of oriented gradients, LBP, and Haralick features. The resulting accuracy has been 87% ± 2%.

Daood et al. [22] have proposed a method that decomposes the images into layers using k-mean clustering, and then performs feature extraction by measuring texture and geometrical characteristics in each layer. Based on SVM classifier they have identified 30 types of pollen grains with classification rate 86.9%.

The aim of this study was to develop an approach for extracting features for the recognition and classification of the pollen of honey plants involved in the most common monofloral honeys in Bulgaria. Geometric (shape and size) and textural (Gabor filter, GLCM, LBP) features were extracted from microscopic images of pollen, which independently or in combination were used in LDA based classifiers. Classification accuracy was determined by leave-one out-cross-validation test.

2. Materials and Methods

To accomplish the goal outlined earlier, the following tasks are described. The study begins by examining the experimental setup, including the methodology, equipment, and chemicals used for collecting the pollen database. Next, the study provides a brief overview of some of the most widely recognized methods for extracting classification features, focusing on those based on image texture as well as those related to pollen geometric shape and size. Following this, two classical methods are selected for processing the obtained classification features: (1) principal component analysis, which is used for reducing dimensionality and eliminating correlations, and (2) linear discriminant analysis, used for supervised classification. Given the limited amount of data, the leave-one-out cross-validation method is chosen as the most suitable for testing the classifiers. Finally, hybrid classifiers that combine textural and geometrical features are proposed. The results section demonstrates that these hybrid classifiers outperform those that use only textural or only geometrical features.

2.1. Light Microscopy based Pollen Image Database

To determine the botanical origin of honey accurately, it is essential to qualitatively and quantitatively analyze its pollen content. Advance preparation of standard pollen samples is necessary to accomplish this task.

Pollen taken from the relevant plant is placed on a glass slide. It is moistened with a drop of distilled water, and after drying, it is fixed with a drop of ethyl alcohol slightly stained with fuchsin. Then the sample is covered with a drop of warmed glycerin-gelatin and a coverslip is carefully placed. After several days, the edges of the cover glass are sealed with Canada balsam. The glycerin-gelatin mixture is obtained from 7g of gelatin mixed with 42 cm^3 of distilled water, to which 50g of glycerin is added. The mixture is heated for 15 minutes and filtered while it is warm. It is heated until is liquefies before use.

A database was compiled with photo images of pollen from the following 5 types of honey plants: acacia (*Robinia Pseudoacacia*), linden (*Tilia Tomentosa*), lavender (*Lavandula Angustifolia*), rapeseed (*Brassica Napus*), and thistle (*Carduus acanthoides*). A ZEISS Primo Star light microscope (magnification x40 of objective) with a ZEISS AxioCam ERc 5s digital camera was used. The images obtained by the camera have a resolution of 2560x1920 pixels, and contained one or several pollens, depending on how many of them fall into the captured area. From these photos, the individual pollens were cut out using the Zeiss ZEN 2.3 lite software, so that an individual photo image containing only one pollen was obtained. Figure 1 shows a mix of single images of the 5 types of pollen, so that the ratio between their actual sizes is preserved. For the presented research, 35 photo images were prepared for each of the 5 types of pollen.
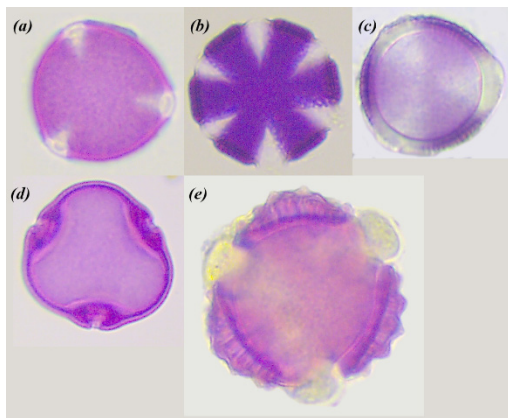

Figure 1. Microscopic image of: acacia - (a); lavender - (b); rapeseed - (c); linden - (d); and thistle - (e)

2.2. Gabor Filter

Some researchers [23] suggest that image analysis using Gabor filters parallels human visual perception. A Gabor filter consists of a Gaussian kernel (elliptical in two dimensions) modulated by a sinusoidal wave [24]. The 2D Gabor filter is presented here as follows:

$$G(x,y) = \exp\left(-\frac{X^2 + \gamma Y^2}{2\sigma^2}\right) \times \cos\left(\frac{2\pi X}{\lambda}\right), \quad (1)$$

where $X = x\cos\theta + y\sin\theta$, $Y = -x\sin\theta + y\cos\theta$. The Gabor filter is characterized by four parameters [25], [26]: orientation, defined by the clockwise angle θ; extent, specified by the width σ of the Gaussian function; spatial frequency, represented by the wavelength λ of the sinusoidal component; and shape, indicated by the spatial aspect ratio γ of the extent in the *X*-direction relative to that in the *Y*-direction.

2.3. Gray Level Co-Occurrence Matrix (GLCM)

Haralick *et al.* [27] have proposed the GLCM as a method for depicting how often different combinations of gray levels co-occur in an image. This matrix shows (Figure 2a) how often a pixel (x, y) with gray intensity value i from the analysed image appears in combination with another pixel $(x + \Delta x, y + \Delta y)$ with reference offset/spatial relationship $(\Delta x, \Delta y)$ and gray intensity with value j. Each element (i, j) in the GLCM is equal to the following sum:

$$C_{\Delta x, \Delta y}(i,j) = \sum_{x=1}^{n} \sum_{y=1}^{m} \begin{cases} 1, & \text{if } I(x,y)=i \text{ and} \\ & I(x+\Delta x, y+\Delta y)=j, \\ 0, & \text{otherwise} \end{cases} \quad (2)$$

where: i, j are the coordinates in the GLCM; x, y are the coordinates in the $(n \times m)$ dimensional image *I*; $(\Delta x, \Delta y)$ is the selected spatial relationship between two pixels; $I(x, y)$ and $I(x + \Delta x, y + \Delta y)$ are the gray level intensity values of the pixels with coordinates (x, y) and $(x + \Delta x, y + \Delta y)$, respectively.
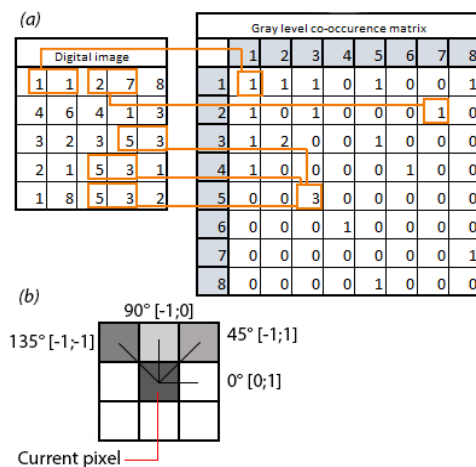

Figure 2. Construction of a gray level co-occurrence matrix – (a); Directions/offsets used to define the spatial relationships of pixels – (b).

In order to the GLCM method be invariant to image rotation, usually it uses 4 spatial relationships $[0\ 1; -1\ 1; -1\ 0; -1\ -1]$ in the form of offsets $(\Delta x, \Delta y)$ of the neighboring pixels, which are respectively at an angle of 0°, 45°, 90° and 135°, relative to the considered pixel (x, y) (Figure 2b).

The number of gray levels N_{GL} in a monochrome photo image I determines the matrix size, e.g. if $N_{GL} = 8$ gray levels the matrix size is 8×8. Certain classification features such as contrast, entropy, homogeneity, correlation, etc. can be extracted from the obtained matrices.

2.4. Local Binary Patterns (LBP)

Ojala et al. [28], [29] have introduced the LBP method as a texture description operator. This approach involves comparing the intensity of the central pixel with the intensities of the surrounding pixels within a small neighborhood. If the intensity of the gray level of the central pixel $I(x_c, y_c)$ is greater than the intensity of its neighbor $I(x_n, y_n)$, 0 is written in the place of the neighbor, otherwise – 1 (Figure 3). The resulting 3×3 matrix is multiplied by a matrix of the same size containing 8 weights by the powers of 2. The values in the resulting matrix are summed and the sum is written at the location of the central pixel. A pattern code is computed by the following:

$$\text{LBP}(x_c, y_c) = \sum_{n=0}^{7} g(I(x_n, y_n) - I(x_c, y_c))2^n, \quad (3)$$

where $g(z) = \begin{cases} 1 & \text{if } z \geq 0 \\ 0 & \text{otherwise} \end{cases}$.

Ojala et al. [30] and Zhao et al. [31] have improved the original LBP operator by placing the neighboring P number of pixels on a circle of radius R. Thus R controls the spatial resolution of the operator, while P - the angular quantization. The sampling points (neighbors) around pixel (x_c, y_c) are calculated as:

$(x_n, y_n) = (x_c + R\cos(2\pi n / P), y_c - R\sin(2\pi n / P))$.

When a sampling point coordinates are not integer ones, the pixel value is bilinearly interpolated.
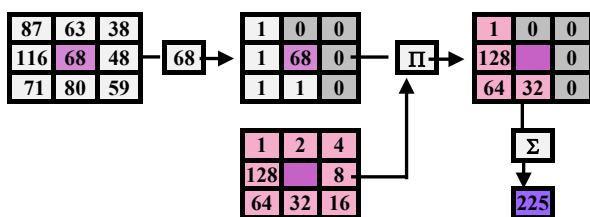

Figure 3. Steps in calculating LBP

2.5. Calculating Geometrical Features (Shape and Size) Using Binary Images

The process of forming a binary image is usually implemented in several steps, depending on the type of the original image. First, the following weighted averaging formula is used to convert a color image to grayscale:

$\text{Gray} = 0.2989\,\text{Red} + 0.5870\,\text{Green} + 0.1150\,\text{Blue} \quad (4)$

The gray image is then converted to a black and white (binary) one. The goal is to separate image into a foreground extracting the important and informative parts of it, and a background containing everything general and insignificant. As a rule, binarization can be divided into global and local one. In global binarization, the entire image is converted based on a single grayscale value applied to the entire image. In the local method different gray threshold values are chosen for each individual pixel on the basis of its neighboring pixels.

Initially a binarizing method specifically oriented to the contour extraction of the pollen shape was proposed in this study. Given that, by definition, each pollen is "cut" from a photographic image of a microscope slide so that it fits into a rectangular region, the corners of that region are very likely included in the background space. The method takes the content of four square regions (e.g., 30x30 pixels) at the corners of the image, converts it to a grayscale image, and calculates the minimum, maximum, and average gray intensities. After experimenting with these three values taken as thresholds, the maximum gray intensity value was selected as the most appropriate for binarization.

Sometimes none of the methods performs well enough on its own, then a hybrid method combining several others (local, global or new custom-made) can be used. In the present study, a hybrid binarization approach is proposed, which on the basis of logical OR sums the binary images obtained by the following 3 methods: (1) Otsu method [32], [33]; (2) Bradley method [34]; and (3) the method described above based on the four corner square regions to determine the binarization threshold.

Once the binary image is obtained, it is possible to extract geometrical features by which the image can be classified. One common method of feature extraction is by defining regions in an image and their associated properties. Regions are a set of connected pixels. The most used properties are [35]:
• Area S – the number of pixels that are contained in the considered region;
• Perimeter P – the distance around the border of the region, represented as a sum of pixels;
• Equivalent diameter D_{eq} – the diameter of a circle that has the same area as the considered region.

- Ovality (Circularity) – calculated according to the following formula:

$$Circularity = \frac{4\pi S}{P^2}\left(1 - \frac{0.5}{r}\right)^2,\qquad(5)$$

where

$$r = \frac{P}{2\pi} + 0.5.$$

- Extent – the ratio of the area of the considered region to the area of the bounding window;
- Eccentricity – the ratio of the distance between the foci of the ellipse to the length of its major axis, where the considered region and the ellipse share the same second moments;
- MinorAxisLength/MajorAxisLength – the length of the minor axis divided by the length of the major axis of an ellipse that has the same normalized second central moments as the region (lengths are measured in pixels);
- MinFeretDiameter/MaxFeretDiameter – the minimum distance between any two boundary points of the antipodal vertices of the convex hull enclosing the object, divided by the maximum distance between such points.

2.6. Multivariate Analysis for Pollen Classification

Multivariate analysis involves techniques by which sets of data are analyzed in the multidimensional space of the variables to find possible associations among them. Generally, the principal component analysis (PCA) is used for data preprocessing, and the linear discriminant analysis (LDA) - for classification in the machine learning algorithms.

PCA is a technique that linearly transforms data from a coordinate system with potentially correlated variables to a new system where the variables are uncorrelated and orthogonal, known as principal components (PCs). The first principal component accounts for the largest variance in the data, the second principal component captures the next largest variance, and so on, up to the final principal component. This method can effectively reduce the dimensionality of the original data by selecting only the most significant principal components that retain a substantial portion of the variance.

LDA is a supervised technique designed to linearly separate two or more classes by maximizing the ratio of between-class variance to within-class variance.

LDA typically demonstrates strong discriminatory power; however, its effectiveness can be diminished in the presence of correlated data or non-linear boundaries between classes.

Features for classification are extracted from pollen images using various techniques, including Gabor filters, GLCM, LBP, and geometric shape and size (either individually or in combination). These features are subsequently processed through PCA and LDA to classify the images into five distinct categories. The performance of the classifiers is evaluated using leave-one-out cross-validation. In this method, one sample (typically the first) is removed from the dataset and used as the test sample, while the remaining samples are employed to train the classifiers. This process is iterated for each sample, ensuring that all samples are tested. Leave-one-out cross-validation is especially advantageous for small datasets.

2.7. The Proposed Hybrid Classifier

Here it is proposed integration of mostly textural classification features (Gabor filter, GLCM, LBP) with geometrical ones (shapes and sizes) to build a hybrid classifier with a higher success rate than the ones that build it. In this way, 3 hybrid classifiers were obtained, combining the eight geometric features with the features extracted from the following methods: (1) Gabor filter; (2) GLCM: (3) LBP. The textural features were processed by the PCA method, which reduced the size of the features and removed the correlation between them. On the basis of the combined features, LDA-based classifiers were built, which were tested by leave-one-out-cross-validation test.

3. Results and Discussion

Multiple microscope slides, each containing pollen from only one species of plant, were prepared and photographed using a light microscope camera. The pollen grains were from honey plants that determine the most common monofloral honeys in Bulgaria: acacia, linden, lavender, rapeseed and thistle (Figure 1). Figure 4 shows a flowchart of the procedure for the synthesis of different pollen classifiers and their testing.

The extracted RGB pollen images were converted to grayscale according to (4). From the gray images, classification features were extracted by the three texture methods: Gabor filters, GLCM, LBP.
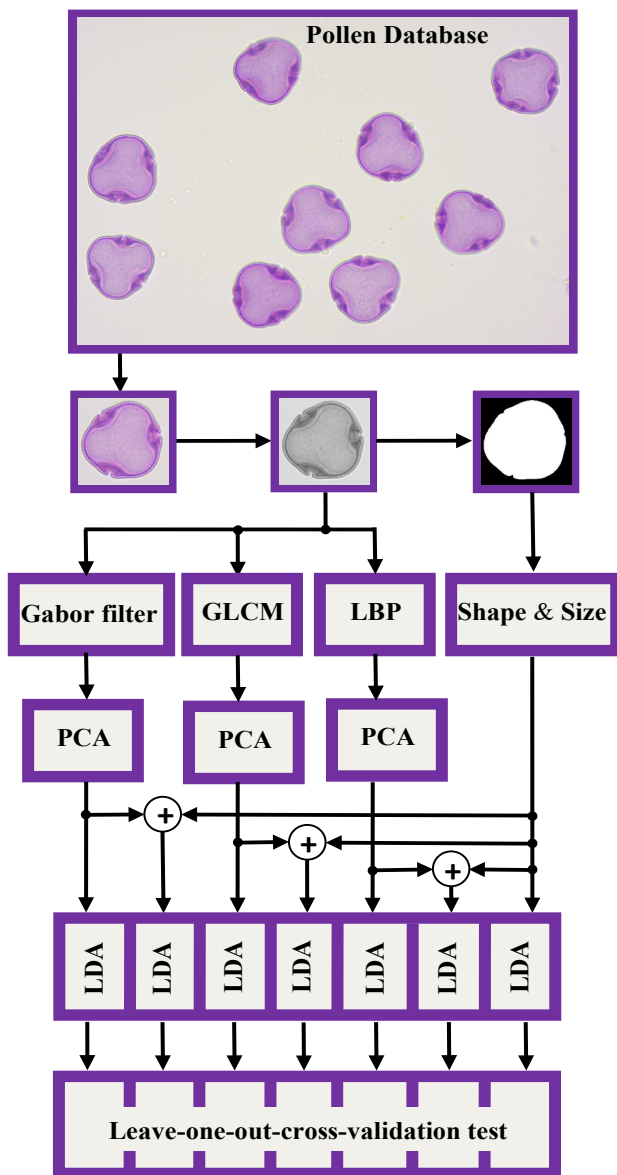
Figure 4. Flowchart of the pollen image classification process

The gray images were then converted to black and white by Otsu method, Bradley method and the custom one. The three images were integrated by logical OR. From the resulting final image, the eight geometric features described in 2.5 were extracted.

All algorithms were implemented using the MATLAB programming environment. The Gabor filter bank was configured using the following parameters: the filter orientation $\theta = 0; 45^0; 90^0; 135^0$, the wavelength of the sinusoidal part $\lambda = 4; 8$, the extent $\sigma = 1$, and the spatial aspect ratio $\gamma = 0.5$. The pollen grains images were reduced to 30 by 30 pixels. Thus, the features vector contained $30 \times 30 \times 8 = 7200$ pixels information. The GLCM method used 8 gray levels and the following 4 spatial relationships: $[0\ 1; -1\ 1; -1\ 0; -1\ -1]$.

The LBP classifier used a set of $P = 8$ members on a circle of radius $R = 1$. The MATLAB implementation did not include rotation invariance.

A total of seven LDA-based classifiers were developed and evaluated using a leave-one-out cross-validation test. Four of these classifiers - Gabor filter, GLCM, LBP, and geometric (Shape & Size (SS)) - are foundational and widely used independently in the literature. The remaining three classifiers represent proposed hybrid variants. The results are summarized in Table 1. Simulations were performed with 1 to 130 principal components for all classifiers except the geometric one. Table 1 presents the optimal results achieved along with the corresponding number of principal components. The geometric classifier utilized all 8 features without PCA processing and yielded the lowest performance at 76.6%. In contrast, the hybrid classifiers GLCM+SS and LBP+SS achieved the highest performance, with accuracy rates of 96%. The GLCM+SS classifier used 9 principal components, while the LBP+SS classifier used 13 principal components.

Table 1. Recognition success rate of the classifiers

Classifier		LDA	
Features		Success, %	Number of Features
Shape & Size	independent	76.57	8
Gabor filter	independent	84.57	30 PCs
	+SS	90.29	30 PCs
GLCM	independent	94.29	21 PCs
	+SS	96.00	9 PCs
LBP	independent	90.29	23 PCs
	+SS	96.00	13 PCs

Table 2 shows the confusion matrix of the GLCM+SS hybrid classifier. It is evident that linden (Tilia) and lavender pollen grains are recognized with 100% accuracy. This is likely due to their distinct shape, which differs significantly from that of other pollen grains. The recognition accuracy for Acacia and Rapeseed pollen grains was the lowest at 91.43%, attributed to their closely similar size and shape. Specifically, one Acacia pollen grain was misclassified as Rapeseed, and two others as Linden. Similarly, two Rapeseed pollen grains were misclassified as Acacia, and one as Linden. Additionally, one Thistle pollen sample was misclassified as Lavender.

Table 2. Confusion matrix of GLCM + SS classifier

4. Conclusion

A hybrid approach was proposed for features extraction in pollen classification, with potential future application to monofloral honey classification. This approach combined features extracted from grayscale microscope photos of pollen grains using Gabor filters, GLCM, and LBP methods, along with geometric features extracted from black and white images. Comparative analysis of seven LDA-based classifiers utilizing textural, geometric, and hybrid features revealed higher success rates for the hybrid classifiers. The proposed modification improved image recognition success rates from 1.8% (hybrid GLCM) to 6.8% (hybrid Gabor filter), with the best result reaching 96% (hybrid GLCM, hybrid LBP). However, computational difficulties may arise with a large number of input features. Future research will explore intelligent classifiers based on artificial neural networks.

Acknowledgements

References:

[1]. Codex Alimentarius Commission Standards. (2001). *Codex Standards for Sugars: Standard 12-1981, Rev. 1, 1987*.

[2]. Council, E. U. (2002). Council Directive 2001/110/EC of 20 December 2001 relating to honey. *Official Journal of the European Communities L, 10*, 47-52.

[3]. Bulgarian Institute for Standardization. (2024). *BDS 2673:1989*. Bulgarian Institute for Standardization. Retrieved from: https://bds-bg.org/bg/project/show/bds:proj:22569 [accessed: 10 June 2024].

[4]. Thrasyvoulou, A., Tananaki, C., Goras, G., Karazafiris, E., Dimou, M., Liolios, V., Kanelis, D., & Gounari, S. (2018). Legislation of honey criteria and standards. *Journal of Apicultural Research, 57*(1), 88-96. Doi:10.1080/00218839.2017.1411181

[5]. Von der Ohe, W., Persano Oddo, L., Piana, M.L., Morlot, M., Martin, P. (2004). Harmonized methods of melissopalynology. *Apidologie, 35*, 18–25. Doi:10.1051/apido:2004050

[6]. Persano Oddo, L., & Bogdanov, S. (2004). Determination of honey botanical origin: Problems and issues. *Apidologie, S35: European unifloral honeys*, 2–3.

[7]. Anklam, E. (1998). A review of analytical methods to determine the geographical and botanical origin of honey. *Food Chemistry, 63*(4), 549-562. Doi: 10.1016/S0308-8146(98)00057-0

[8]. Hermosín, I., Chicón, R. M., & Cabezudo, M. D. (2003). Free amino acid composition and botanical origin of honey. *Food Chemistry, 83*(2), 263-268. Doi: 10.1016/S0308-8146(03)00089-X

[9]. Mateo R., & Bosch-Reig F. (1998). Classification of Spanish Unifloral Honeys by Discriminant Analysis of Electrical Conductivity, Color, Water Content, Sugars, and pH. *Journal of Agricultural and Food Chemistry, 46*(2), 393-400. Doi: 10.1021/jf970574w

[10]. Vlaeva, I., Nikolova, K, Bodurov, I., Marudova, M., Tsankova, D., Lekova, S., Viraneva, A., & Yovcheva, T. (2017). Using differential scanning calorimetry, laser refractometry, electrical conductivity and spectrophotometry for discrimination of different types of Bulgarian honey. *In (ISCMP) IOP Conf. Series: Journal of Physics: Conf. Series 794*. Doi: 10.1088/1742-6596/794/1/012034

[11]. Li, Y., & Yang, H. (2012). Honey Discrimination Using Visible and Near-Infrared Spectroscopy. *International Scholarly Research Network, ISRN Spectroscopy,* 487040, Doi:10.5402/2012/487040

[12]. Tsankova, D., Lekova, S. (2015). Botanical Origin-Based Honey Discrimination Using Vis-NIR Spectroscopy and Statistical Cluster Analysis. *Journal of Chemical Technology and Metallurgy (JCTM), 50*(5), 638-642. University of Chemical Technology and Metallurgy, BG

[13]. Nankov, K., Tsankova, D., & Terziyski, G. (2019). UV-VIS Spectroscopy and Neural Networks in Distinguishing Different Types of Honey. *Proceedings of the IX International Conference Industrial Engineering and Environmental Protection (IIZS 2019), Zrenjanin, Serbia*, 86-93. ISBN: 978-86-7672-324-9

[14]. Lekova, S., & Tsankova, D. (2017). Determination of botanical origin of honey by mid infrared spectroscopy (mid-FTIR), colorimetry and chemometric analysis. *J. Chem. Technol. Metall*, *52*, 52-57.

[15]. Nikolova, K., Tsankova, & D., Evtimov, T. (2015). Fluorescence Spectroscopy, Colorimetry and Neural Networks in Distinguishing Different Types of Honey. *V International Conference Industrial Engineering and Environmental Protection 2015 (IIZS 2015), Zrenjanin, Serbia,* 317-322.

[16]. Treloar, W. J., Taylor, G. E., & Flenley, J. R. (2004). Towards automation of palynology 1: analysis of pollen shape and ornamentation using simple geometric measures, derived from scanning electron microscope images. *Journal of Quaternary Science (J. Quaternary Sci.), 19*(8), 745-754. John Wiley & Sons, Ltd., Doi: 10.1002/jqs.871

[17]. García, N. M., Chaves, V. A. E., Briceño, J. C., & Travieso, C. M. (2012). Pollen grains contour analysis on verification approach. In *Hybrid Artificial Intelligent Systems: 7th International Conference, HAIS 2012, Salamanca, Spain, March 28-30th, 2012. Proceedings, Part I 7*, 521-532. Springer Berlin Heidelberg.

[18]. Marcos, J. V., Nava, R., Cristóbal, G., Redondo, R., Escalante-Ramírez, B., Bueno, G., Déniz, Ó., González-Porto, A., Pardo, C., Chung, F., & Rodríguez, T. (2015). Automated pollen identification using microscopic imaging and texture analysis. *Micron, 68*, 36–46,
Doi: 10.1016/j.micron.2014.09.002

[19]. Kaya, Y., Erez, M. E., Karabacak, O., Kayci, L., & Fidan, M. (2013). An automatic identification method for the comparison of plant and honey pollen based on GLCM texture features and artificial neural network. *Grana, 52*(1), 71-77.
Doi: 10.1080/00173134.2012.754050

[20]. Rodrıguez-Damian, M., Cernadas, E., Formella, A., Fernandez-Delgado, M., & De Sa-Otero, P. (2006). Automatic Detection and Classification of Grains of Pollen Based on Shape and Texture. *IEEE Transactions on Systems Man and Cybernetics, Part C (Applications and Reviews), 36*(4).
Doi: 10.1109/TSMCC.2005.855426

[21]. Chudyk, C., Castaneda, H., Leger, R., Yahiaoui, I., & Boochs, F. (2015). Development of an automatic pollen classification system using shape, texture and aperture features. In *LWA 2015 Workshops: KDML, FGWM, IR, and FGDB*, 1458, 65-74.

[22]. Daood A., Ribeiro E., & Bush M. (2016). Pollen Recognition Using Multi-Layer Feature Decomposition. *Proceedings of the Twenty-Ninth International Florida Artificial Intelligence Research Society Conference*, 26-31. Association for the Advancement of Artificial Intelligence.

[23]. Daugman, J. G. (1985). Uncertainty relation for resolution in space, spatial frequency, and orientation optimized by two-dimensional visual cortical filters. *Journal of The Optical Society of America A-optics Image Science and Vision (Optical Society of America), 2*(7), 1160-1169.
Doi: 10.1364/josaa.2.001160.

[24]. Jones, J.P., & Palmer, L.A. (1987). An evaluation of the two-dimensional Gabor filter model of simple receptive fields in cat striate cortex. *Journal Neurophysiology, 58*(6), 1233-1258.
Doi: 10.1152/jn.1987.58.6.1233

[25]. Hamilton, W. (2013). *Biologically Inspired Object Recognition using Gabor Filters*. cim.mcgill.ca Retrieved from:
https://www.cim.mcgill.ca/~siddiqi/COMP-558-2012/willhamilton.pdf
[accessed: 02 June 2024]

[26]. Nikolov, D.N., & Tsankova, D.D. (2018). Features Extraction for Pollen Recognition in Honey Using Gabor Filters. *Food Science and Applied Biotechnology, 1*(2), 86-95.
Doi: 10.30721/fsab2018.v1.i2.

[27]. Haralick R.M., Shanmugam, K., & Dinstein, I. (1973). Textural Features for Image Classification. IEEE Trans. *On Systems, Man and Cybernetics*, 610-621.

[28]. Ojala, T., Pietikäinen, M, & Harwood, D. (1994). Performance evaluation of texture measures with classification based on Kullback discrimination of distributions. *Proceedings of the 12th IAPR International Conference on Pattern Recognition (ICPR 1994), 1*, 582 - 585.

[29]. Ojala, T., Pietikainen, M., & Harwood, D. (1996). A Comparative Study of Texture Measures with Classification Based on Feature Distributions. *Pattern Recognition, 29*, 51-59.
Doi: 10.1016/0031-3203(95)00067-4

[30]. Ojala, T., Pietikainen, M., & Maenpaa, T. (2002). Multiresolution Gray Scale and Rotation Invariant Texture Classification With Local Binary Patterns. *IEEE Transactions on Pattern Analysis and Machine Intelligence, 24*(7), 971-987.

[31]. Zhao, G., Ahonen, T., Matas, J., & Pietikäinen, M. (2012). Rotation-Invariant Image and Video Description With Local Binary Pattern Features. *IEEE Transactions on Image Processing, 21*(4), 1465-1477.

[32]. Otsu, N. (1979). A Threshold Selection Method from Gray-Level Histograms. *IEEE Transactions on Systems, Man, and Cybernetics, 9*(1), 62-66.
Doi: 10.1109/TSMC.1979.4310076

[33]. Bangare, S. L., Dubal, A., Bangare, P. S., & Patil, S. (2015). Reviewing Otsu's method for image thresholding. *International Journal of Applied Engineering Research*, *10*(9), 21777-21783.

[34]. Bradley, D., & Roth, G. (2007). Adapting Thresholding Using the Integral Image. *Journal of Graphics Tools, 12*(2), 13–21.

[35]. The MathWorks. (n.d.). *MATLAB: Image Processing Toolbox*. The MathWorks, Inc. Retrieved from:
https://www.mathworks.com/products/image-processing.html [accessed: 03 June 2024].